Dyes and Pigments 149 (2018) 566–573

Contents lists available at ScienceDirect

Dyes and Pigments

journal homepage: www.elsevier.com/locate/dyepig

Theoretical and experimental studies of aryl-bithiophene based push-pull π-conjugated heterocyclic systems bearing cyanoacetic or rhodanine-3-acetic acid acceptors for SHG nonlinear optical applications

Sara S.M. Fernandes[a], Cyril Herbivo[a], João Aires-de-Sousa[b], Alain Comel[c], Michael Belsley[d], M. Manuela M. Raposo[a,*]

[a] Centro de Química, Universidade do Minho, Campus de Gualtar, 4710-057 Braga, Portugal
[b] LAQV e Departamento de Química, Faculdade de Ciências e Tecnologia, Universidade Nova de Lisboa, 2829-516 Caparica, Portugal
[c] Université de Lorraine, Institut Jean Barriol, Laboratoire de Chimie et Physique - Analyse Multi-échelles des Milieux Complexes, F-57048 Metz Cedex, France
[d] Centro de Física, Universidade do Minho, Campus de Gualtar, 4710-057 Braga, Portugal

ARTICLE INFO

Keywords:
Arylbithiophene
Cyanoacetic acid
Rhodanine-3-acetic acid
Density functional theory (DFT)
Nonlinear optics
Second harmonic generation (SHG)

ABSTRACT

A series of push-pull aryl-bithiophene based systems **2–3** were designed and synthesized in order to understand how structural modifications influence the electronic, linear and nonlinear optical properties. The push-pull conjugated chromophores **2–3** bear a bithiophene spacer conjugated with a phenyl ring functionalized with *N,N*-dialkylamino electron-donor groups together with cyanoacetic or rhodanine-3-acetic acid acceptor groups. Theoretical (DFT calculations) and experimental studies were carried out to obtain information on conformation, electronic structure, electron distribution, dipolar moment, and molecular nonlinearity response of the push-pull bithiophene derivatives. This multidisciplinary study revealed that chromophore **2e** exhibits the highest value for hyperpolarizability β (10440 $\times$ 10^{-30} esu) due to the strong electron donating ability of the *N,N*-dimethylamino group, and the ethyne linker that not only lengthens the π-conjugation path but also grants less distortion to the system.

1. Introduction

For the last several years, push-pull π-conjugated systems have attracted widespread interest. The D-π-A molecular arrangement of these systems allows the electron donor and acceptor end-caps to interact through a π-conjugated spacer, facilitating intramolecular charge-transfer (ICT) upon visible light excitation (colored substances). The large polarizability and often large difference between the molecular dipole moments in the ground and first excited electronic state of this push-pull chromophores favor strong nonlinear optical responses. Such compounds are especially noteworthy due to their easy synthesis, excellent optical and electrochemical properties, well-defined structures that can easily be tuned to satisfy various requirements, as well as their good thermal and chemical stability [1]. Practical applications are found in various areas, including field-effect transistors (OFETs) [2], light emitting diodes (OLEDs) [3], nonlinear optics (SHG, TPA) [4], photovoltaic cells (OPVCs) [5], dye-sensitized solar cells (DSSCs) [6], bulk heterojunction cells (BHJs) [7], near infrared absorbing (NIR) dyes [8], etc. Due to the great interest in these types of systems, an extensive catalog of electron donor, electron acceptor and π-spacer groups have already been studied for the preparation of push-pull chromophores.

In principle, the NLO response of an organic push-pull system depends on the number of polarizable π-electrons, the extent of the ICT, the polarization of the given π-system by suitable and strong electron donors and acceptors and the overall planarity [1b,9]. The tuning of such molecular systems to adjust the respective properties for the desired applications can be achieved through modification of the electron donor or electron acceptor moieties, modification of the spacer (electronic nature and relative position of the aromatic or heteroaromatic rings, conjugation length), and varying the overall chromophore arrangement (planarity, and further auxiliary functionalization).

Among the numerous classes of π-conjugated organic systems, donor-acceptor substituted heterocyclic compounds are of great interest because it has been experimentally and theoretically demonstrated that they increase the second-order molecular NLO response of push-pull chromophores with respect to aryl analogues. The incorporation of heterocycles into the π-conjugated systems is a powerful approach for tuning the optoelectronic properties. The heterocycles bring higher polarizability, modulate the conjugation pathway, promote thermal and chemical robustness, and behave as auxiliary electron donors/

* Corresponding author.
E-mail address: mfox@quimica.uminho.pt (M.M.M. Raposo).

http://dx.doi.org/10.1016/j.dyepig.2017.10.001
Received 24 August 2017; Received in revised form 27 September 2017; Accepted 1 October 2017
Available online 03 October 2017
0143-7208/

acceptors, while constituting moieties for further modification [9a,10]. Functional oligothiophenes are one of the most frequently used π-conjugated materials for active components in organic devices due to their enhanced stability, excellent charge-transport properties, and large nonlinearities that can be attributed not only to the bathochromic effect of sulfur, but also to the partial decrease of aromatic character and the increased π-overlap between the thiophene units [4b,9b-d,10a-h,11].

Motivated by previous studies, as well as our experience in the design, synthesis and characterization of push-pull heterocyclic π-conjugated systems bearing (bi)thiophene spacers for a variety of nonlinear optical [10] photovoltaic [12] and photochromic applications [13], here we report on theoretical and experimental studies of ten arylbithiophene-based push-pull heterocyclic systems. These NLOphores bear cyanoacetic or rhodanine-3-acetic acid as electron withdrawing group [14], and *N,N*-dialkylamino donor groups, with the aim of improving their second harmonic generation efficiency.

2. Results and discussion

2.1. Design of arylbithiophene-based derivatives 1-3

Motivated by the several interesting characteristics stated above, we designed and synthesized ten push-pull heterocyclic systems, from which eight are new compounds, based on an aryl-bithiophene spacer/auxiliary donor, and cyanoacetic acid or rhodanine-3-acetic acid as electron acceptor moieties in order to study their performance as second harmonic generators (SHG) (Fig. 1). The final push-pull systems were obtained by transformation of the versatile formyl heterocyclic precursors **1a-e**, reported recently by our research group [15], to the cyanoacetic acid **2a-e**, or rhodanine-3-acetic acid **3a-d** derivatives. These molecular structures permit a comparative study of the optical properties among the different chosen electron donor, electron-acceptor groups, as well as the introduction of an ethyne linker (Scheme 1).

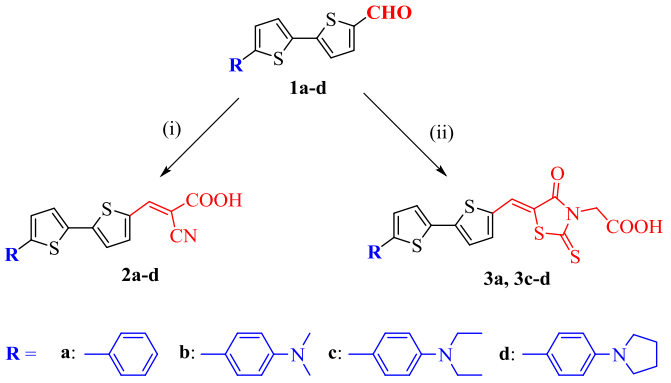

Scheme 1. Synthesis of push-pull arylbithiophene dyes **2a-d**, **3a** and **3c-d**: (i) 2-cyanoacetic acid, acetonitrile, piperidine, reflux; (ii) rhodanine-3-acetic acid, ethanol, piperidine, reflux.

2.2. Theoretical calculations for arylbithiophene-based derivatives 2–3

In order to achieve an understanding of the differences in the structure and electronic properties of these dyes, and establish a comparative computational basis for this series, density functional theory (DFT) calculations were undertaken. The obtained results are summarized in Table 1 and Fig. 2. The energy levels for chromophores **2–3**, and the respective electron density maps were computed in a polarized solvent continuum of 1,4-dioxane. In addition, their dipolar moments and hyperpolarizabilities β were calculated.

Each chromophore can exist as several different conformers, depending on the relative arrangement of some of their units, however we only present the lowest energy forms, which are responsible for the respective properties. For all the presented conformers, the cyano and the carboxylic groups, as well as the rhodanine moiety, are coplanar with the bithiophene spacer, showing a strong conjugation between the π-orbitals of the aforementioned groups, which translates into efficient electron transfer from the π-bridge to the electron acceptor group (Fig. 2).

The HOMO of chromophores **2–3** is essentially localized on the functionalized arylbithiophene donor group/π-spacer. The electron density of the LUMO for cyanoacetic chromophores **2** is localized on the cyano and carboxylic group with some overflow to the arylbithiophene spacer. For chromophores **3**, the LUMO is mainly centered on the rhodanine heterocycle with some overflow to the arylbithiophene spacer, and isolated from the carboxylic endcap group [12b,d,14].

A comparison of the energy levels of the HOMO and LUMO of the chromophores, shows that the substitution of the cyanoacetic group for the rhodanine-3-acetic acid leads to a stabilization of the LUMO with a destabilization of the HOMO, resulting in the decrease of the electrochemical band gap, and justifying bathochromic shifts of the wavelength of maxima absorption. The stronger electron donor ability of the *N,N*-dialkylamino groups also results in smaller band gaps for chromophores **2b-d** and **3b-d** compared to the unsubstituted derivatives **2a** and **3a**. Comparison of the band gap values for cyanoacetic derivatives **2b** (2.37 eV) and **2e** (2.25 eV) shows that the introduction of an ethyne linker between the bithiophene spacer and the functionalized aryl group also decreases the band gap due to an additional increase of the π-conjugation and an increase of the planarization of the conjugated system.

The calculated dipole moments, in 1,4-dioxane, for chromophores **2–3** are in the range of 5.7–12.5 Debye. As expected, a general increase of the dipole moment with the strength of the electron donating or withdrawing ability of the donor or acceptor groups, was observed for compounds **2–3**. The estimation of the hyperpolarizabilities $\beta_{||}$ and β_{tot} for the designed systems **2–3** gave moderate to high values of 192-2255 × 10^{-30} esu and 320-3757 × 10^{-30} esu, respectively, and generally follows the same trend as the DFT calculated dipole moments. One exception lies in chromophores **2e** and **3e**: the presence of the ethyne linker significantly increases the hyperpolarizability, probably

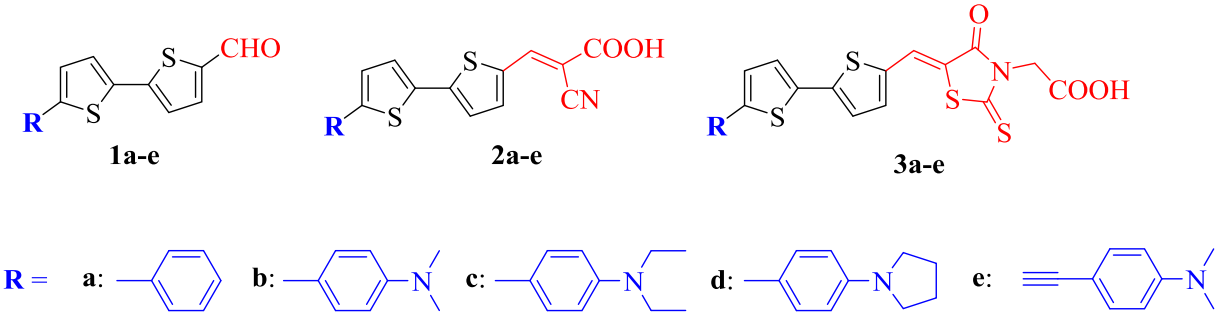

Fig. 1. Molecular structure of the designed push-pull heterocyclic systems **1–3** bearing an aryl-2,2′-bithiophene spacer moiety.

Table 1
Computational result summary of chromophores **2a-e** and **3a-e** hyperpolarizability calculations.

Cpds	μ (D)	$\beta_{\|\|}$ (10^{-30} esu)	β_{tot}(10^{-30} esu)	E_{HOMO} (eV)	E_{LUMO} (eV)	E_g (eV)
2a	6.28	192	320	−5.87	−3.01	2.86
2b	11.70	950	1582	−5.23	−2.86	2.37
2c	11.79	1036	1726	−5.20	−2.86	2.35
2d	12.46	1104	1840	−5.17	−2.85	2.32
2e	12.25	1688	2813	−5.22	−2.97	2.25
3a	5.72	277	461	−5.69	−3.01	2.68
3b	11.10	1383	2302	−5.16	−2.89	2.27
3c	11.24	1529	2546	−5.13	−2.88	2.25
3d	11.94	1647	2743	−5.10	−2.87	2.23
3e	11.49	2255	3757	−5.16	−2.98	2.18

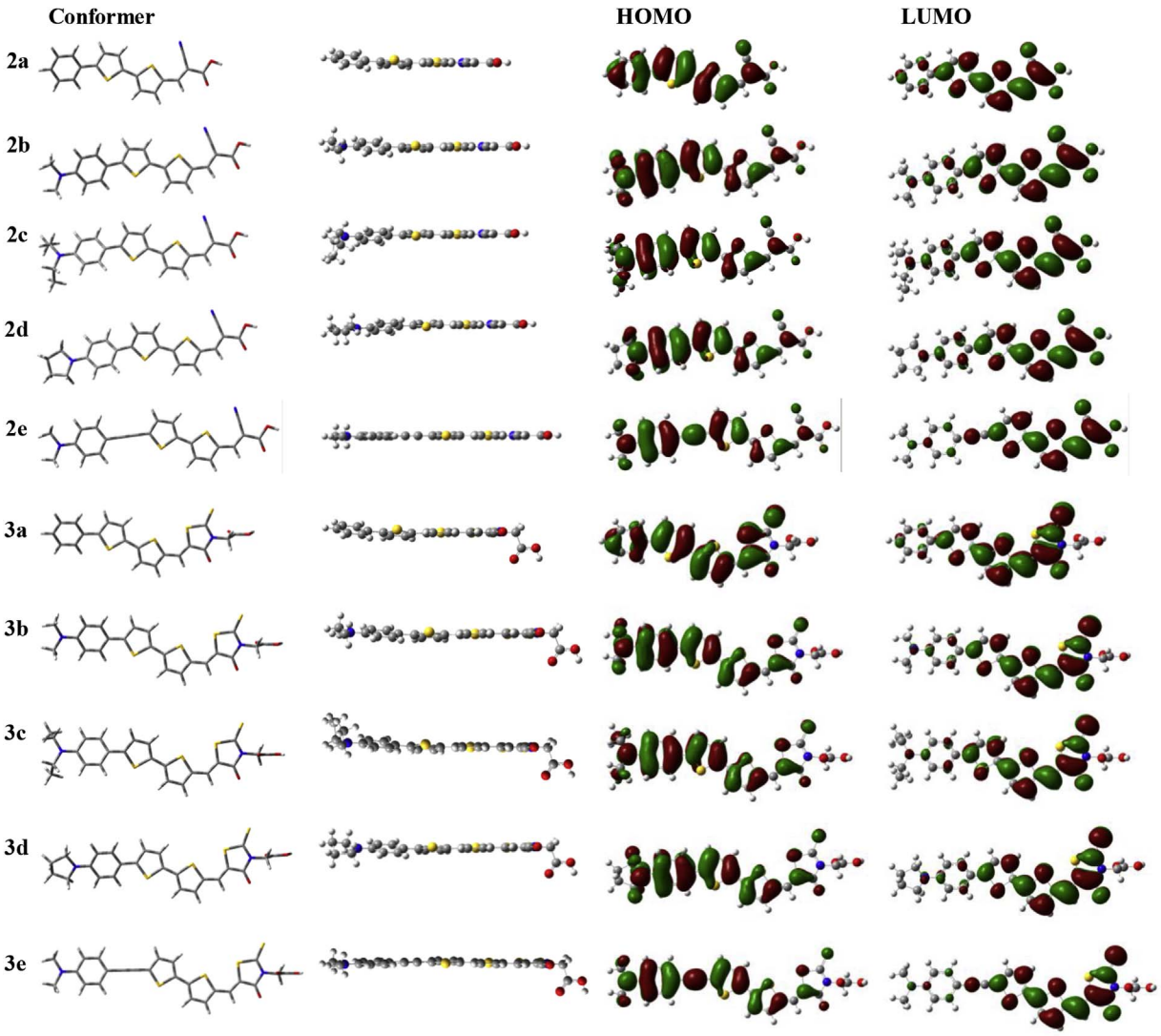

Fig. 2. Optimized geometry of the lowest energy conformer, and frontier molecular orbitals of aryl-bithiophene derivatives **2–3**.

due to a longer conjugation path length. Nevertheless, this has a weak influence on the dipole moment, for which the *N,N*-dialkylamino groups are more relevant. Moreover, the cyanoacetic acid derivatives **2** exhibit stronger dipole moments when compared to the respective analogous rhodanine-3-acetic acid derivatives **3**, while the latter show higher hyperpolarizabilities. This can be ascribed to the fact that the cyanoacetic acid group has a stronger electron withdrawing ability, whereas the rhodanine-3-acetic acid moiety has longer π-conjugation.

The overall analysis of the computational calculations gives reason to believe that these chromophores can be excellent candidates as SHG chromophores.

*2.3. Synthesis and characterization of arylbithiophene-based derivatives **2-3***

Earlier we reported the synthesis and evaluation of the linear and nonlinear optical properties for several families of push-pull thiophene derivatives [10a-h, 13, 15]. Our earlier work, as well as the DFT

Table 2
Yields, IR and ^{1}H NMR data for push-pull arylbithiophene dyes **2a-d**, **3a** and **3c-d**.

Cpds	η (%)	IR[a] ν (cm^{-1})			^{1}H NMR[b] δ (ppm)		
		C=O	O-H	C≡N	C=S	=C*H*$_{vinylic}$	C*H*$_2$
2a	81	1658	3335	2207	–	8.64	–
2b	40	1655	–	2199	–	8.03	–
2c	50	1635	–	2201	–	8.03	–
2d	75	–	–	–	–	8.03	–
3a	69	1581	3360	–	1275	8.10	4.52
3c	24	1585	3363	–	1279	8.09	4.56
3d	38	1585	3366	–	1281	8.07	4.49

[a] IR spectra for compounds **2a-d** were performed in nujol, and in liquid film for compounds **3a** and **3c-d**.

[b] ^{1}H NMR spectra for compounds **2a-d** were performed in $CDCl_3$, and DMSO-d_6 for compounds **3a** and **3c-d**.

calculations presented above for new arylbithiophene derivatives bearing cyanoacetic acid and rhodanine-3-acetic acid acceptor groups, motivated us to extend our studies in order to explore the effect of these different electron acceptor groups as well as the introduction of an ethyne linker on the optical properties of the novel push-pull systems.

Therefore, we synthesized push-pull cyanoacetic acids **2**, and rhodanine derivatives **3**, in order to evaluate their experimental linear and nonlinear optical properties. The synthesis of arylbithiophene-2-carbaldehyde precursors **1a-d** [15] and **1e** [12b,16] were reported by us elsewhere, as were cyanoacetic derivative **2e** [12b,16] and rhodanine-acetic derivative **3b** [11b]. Compounds **2a-d**, **3a** and **3c-d** were prepared in fair to good yields (24–81%) by Knoevenagel condensation of the corresponding aldehydes **1a-d** with 2-cyanoacetic acid in refluxing acetonitrile, or rhodanine-3-acetic acid in refluxing ethanol, and using piperidine as catalyst (Scheme 1, Table 2).

The structures of the push-pull heterocyclic compounds **2–3** were confirmed by standard analytical and spectroscopic techniques. The most characteristic signals in the IR spectra of compounds **2a-d** are the carbonyl (1635-1658 cm^{-1}), and nitrile (2199-2207 cm^{-1}) groups. ^{1}H NMR spectroscopy was also used to identify the singlet that corresponds to the vinylic proton of the ethylenic bridge (C=C*H*) linked to the cyanoacetic acid moiety at $\delta \sim$ 8.03–8.64 ppm. The most characteristic signals in the ^{1}H NMR spectra of compounds **3a** and **3c-d** are a singlet corresponding to the vinylic proton of the ethylenic bridge linked to the rhodanine-3-acetic acid moiety at $\delta \sim$8.07–8.10 ppm; and a singlet at $\delta \sim$4.49–4.56 ppm that corresponds to the C*H*$_2$ protons of the acetic acid unit. IR spectroscopy was also used to identify the typical absorption bands, the carbonyl (1581-1585 cm^{-1}), the hydroxyl (3360-3366 cm^{-1}), and the thiocarbonyl (1275-1281 cm^{-1}) groups of the rhodanine-3-acetic acid moiety.

2.4. Study of the linear and nonlinear optical properties of arylbithiophene-based derivatives *2a-e* and *3a-d*

The optical properties of push-pull heterocyclic compounds **2a-e** and **3a-d** were investigated in 1,4-dioxane and/or ethanol at room temperature, and the experimental data are presented in Fig. 3 and in Table 3. All push-pull chromophores **2a-e** and **3a-d** exhibit a strong and broad band absorption (in 1,4-dioxane) between 430 and 494 nm that can be assigned to an internal charge transfer transition (ICT) between the electron donor and acceptor groups through the π-spacer, which is dependent on the electronic strength of the donor groups. Generally, greater π-conjugation length, stronger electron donating ability of the donor moiety, stronger electron withdrawing ability of the acceptor group, and longer alkyl chains, all induce bathochromic shifts in the wavelength of absorption maxima of the π-conjugated molecules. The substitution of the cyanoacetic acid acceptor moiety for the rhodanine-3-acetic acid, introduces longer π-conjugation onto the systems,

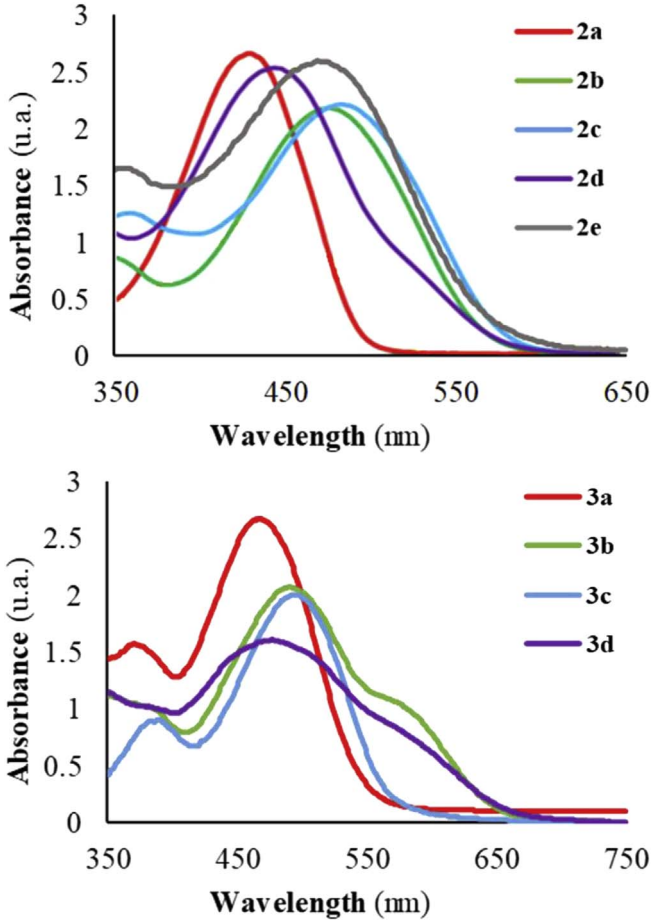

Fig. 3. Absorption spectra of cyanoacetic acid based dyes **2a-e** and rhodanine-3-acetic acid based dyes **3a-d**, in 1,4-dioxane.

inducing bathochromic shifts of about 20–28 nm. The introduction of *N,N*-dialkylamino groups in position 4- of the phenyl moiety, again leads to bathochromic shifts (20–44 nm), due to its higher electron donating ability, as do the longer ethyl chain (**2c** and **3c**) when compared to the methyl group (**2b** and **3b**) (5–8 nm). On the other hand, the cyclized pyrrolidino group induces hypsochromic shifts in the range of 17–25 nm (**2d** and **3d**) relative to the analogous *N,N*-diethylamino moiety (**2c** and **3c**). These results are in agreement with the estimated band gap values for the chromophores. The novel compounds **2a-e** and **3a-d** exhibit molar extinction coefficients in the range of 10,794–27,249 M^{-1} cm^{-1}.

The push-pull dyes **2e** and **3a-d** were excited at the wavelength of maximum absorption in ethanol, at room temperature, to study their fluorescence properties (Table 3). The nature of the donor and acceptor groups significantly influences their emissive properties. Generally, an increase in the extent of the π-electron system (degree of conjugation) or substitution with stronger electron donor or acceptor groups leads to a shift of the spectra to longer wavelengths. Arylbithiophenes **2e** and **3a-d**, display emission peaks at 621, 533, 663, 671, and 582 nm, respectively. The emission spectra of compounds **3a-d** followed the same trend described for the absorbance. A bathochromic shift of the λ_{em} of the compounds is observed for dyes **3a-c** that can be attributed to the increasing electron donating ability of the donor groups (phenyl < *N,N*-dimethylanilino < *N,N*-diethylanilino). Moreover, a comparison of the fluorescence properties between dyes **2e** and **3b** show that the loss of the ethynyl linker, and the additional substitution of the cyanoacetic acid acceptor group by the rhodanine-3-acetic acid moiety, leads to a bathochromic shift that is ascribed to the longer π-conjugation of dye **3b**. We have estimated the optical HOMO-LUMO gap as the

Table 3
UV-vis absorption and emission data in 1,4-dioxane and/or ethanol, β and β_0 values for chromophores **2a-e** and **3a-d**.

Cpds	Ethanol					1,4-Dioxane				
	λ_{max} (nm)	ε (M^{-1} cm^{-1})	λ_{em} (nm)	Φ_F	Stokes' Shift (nm)	λ_{max} (nm)	ε (M^{-1} cm^{-1})	ΔE^{opt} (eV)	β [a,b] (10^{-30} esu)	βo [b,c] (10^{-30} esu)
2a	–	–	–	–	–	430	**27,249**	2.44	325	94
2b	–	–	–	–	–	466	21,008	2.02	4270	800
2c	–	–	–	–	–	474	20,661	2.01	9870	1630
2d	–	–	–	–	–	449	22,523	2.05	[d]	–
2e	452	35,323	621	0.05	169	469	26,808	2.07	10440	1875
3a	450	23,667	533	0.05	81	467	25,542	2.23	2585	480
3b	479	14,877	663	0.08	184	489	15,016	1.89	5150	630
3c	489	13,505	671	0.22	182	494	14,259	2.07	7300	790
3d	469	11,787	582	0.27	113	477	10,794	1.86	[d]	–
***p*NA**	–	–	–	–	–	352	–		40.1	20.1

[a] Experimental first hyperpolarizabilities β and spectroscopic data measured in dioxane solutions.
[b] All compounds are transparent at the 1064 nm fundamental wavelength and the hyperpolarizability values are reported using the T-convention.
[c] Data corrected for resonance enhancement at 532 nm using the two-level model with $\beta_0 = \beta\ [1-(\lambda_{max}/1064)^2][1-(\lambda_{max}/532)^2]$; damping factors not included 1064 nm.
[d] Due to overlapping fluorescence it was not possible to measure the β value.

energy corresponding to the onset of absorption and included these values in Table 3. These values are consistently lower than computational results quoted in Table 1, but follow the same general trends. All dyes exhibit weak emissive properties, with relative fluorescence quantum yields ranging from 0.05 to 0.27, which can be due to the nitrogen heteroatom being involved in the π-system. In these situations, the n→π* transition may be the lowest lying transition, which is characterized by a longer radiative lifetime than that of low lying π→π* transitions. Such a slow process cannot compete with the dominant non-radiative processes, explaining the low fluorescence quantum yields of many compounds containing carbonyl and/or nitrogen based groups [17]. All push-pull systems exhibit large Stokes shifts in the range of 83–184 nm.

The molecular first hyperpolarizabilities β of push-pull bithiophene derivatives **2a-d** and **3a-d** were obtained by the hyper-Rayleigh scattering (HRS) technique [18] at a fundamental wavelength of 1064 nm of a Nd:YAG Q-switched pulsed laser beam. Dioxane was used as the solvent, and the β values were measured against a reference solution of *p*-nitroaniline (*p*NA) [19] in order to obtain quantitative values, while care was taken to properly account for possible fluorescence of the dyes (see experimental section for more details). The static hyperpolarisability β_0 values [20] were calculated using a very simple two-level model neglecting damping. They are therefore only indicative and should be treated with caution.

From Table 3 it is noticeable that the longer π-conjugation and the progression of the electronic donating/withdrawing ability of the donor/acceptor groups, respectively, have a clear influence on the nonlinearities of compounds **2a-c**, **2e** and **3a-c**. The results show an enhancement of the hyperpolarizabilities β from R = H ($\beta = 325 \times 10^{-30}$ esu for **2a**, $\beta = 2585 \times 10^{-30}$ esu for **3a**) to the *N,N*-dimethylamino group ($\beta = 4270 \times 10^{-30}$ esu for **2b**, $\beta = 5150 \times 10^{-30}$ esu for **3b**), and then to a *N,N*-diethylamino group ($\beta = 9870 \times 10^{-30}$ esu for **2c**, $\beta = 7300 \times 10^{-30}$ esu for **3c**). Generally, higher hyperpolarizabilities were also observed for rhodanine derivatives **3**, when compared to chromophores **2** that can be attributed to the longer π-conjugation of the system introduced by the rhodanine-3-acetic acid acceptor moiety. Chromophore **2e** showed the highest first hyperpolarizability β value of all synthesized derivatives. This result can be explained not only by the longer π-conjugation, but also to the less distortion of the system brought by the ethyne linker when compared to chromophores **2b-c**. In fact, comparison of the hyperpolarizability β between **2b** (4270×10^{-30} esu) and **2e** (10440×10^{-30} esu) shows that the introduction of the ethyne linker alone induces an increase of the hyperpolarizability β value by more than the double.

Due to a strong signal from overlapping fluorescence, it was not possible to measure the β value for chromophores **2d** and **3d**.

3. Conclusions

Starting from previously prepared aldehyde precursors, arylbithiophene chromophores **2a-e** and **3a-d** were obtained in good to fair yields, by Knoevenagel condensation.

Experimental and theoretical studies concerning the optical and electronic properties were performed in order to study the effect of different electron donor and acceptor groups as well as a different linker on the arylbithiophene push-pull systems. These comparative studies demonstrated that the substitution of the cyanoacetic acid for the rhodanine-3-acetic acid acceptor introduces longer π-conjugation into the system and enhances the internal charge transfer of the molecules. The same was observed with the increase of the electron donating ability, by introducing different *N,N*-dialkylamino groups to the phenyl ring. The highest hyperpolarizability β value obtained was 10440×10^{-30} esu for **2e**, due to a combination of strong electron donating ability of the *N,N*-diethylamino group, and long conjugation path length brought by the ethyne linker. Further tuning of the molecular structure of all chromophores is likely to produce further enhanced hyperpolarizabilities.

4. Experimental

4.1. Theoretical calculations

All theoretical calculations were performed in Gaussian 09 [21]. The geometry of each molecule was optimized using the density functional theory (DFT) at the B3LYP level by employing the 6-311G** basis set and using polarizable continuum model with dioxane as the solvent. [keyword: SCRF = (PCM,Solvent = 1,4-Dioxane)]. Frequency calculations were performed to ensure the absence of negative frequencies. Hyperpolarizability factors were estimated at the same level of theory using an incident wavelength of 1064 nm (keywords: freq = raman, cphf = rdfreq, polar) and with a polarized solvent continuum model using dioxane as the solvent.

4.2. Materials and methods

2-Cyanoacetic acid was purchased from Aldrich. Rhodanine-3-acetic acid was purchased from Alfa Aesar. All commercially available reagents and solvents were used as received. The synthesis of the

arylbithiophene-2-carbaldehyde precursors **1a-d** [15] and **1e** [12b,16] are reported elsewhere, as is cyanoacetic derivative **2e** [12b,16] and rhodanine-acetic dericivative **3b** [12b]. Reaction progress was monitored by thin layer chromatography, using 0.25 mm thick precoated silica plates (Merck Fertigplatten Kieselgel 60 $F^{25}4$), and spots were visualized under UV light. Purification was achieved by silica gel column chromatography (Merck Kieselgel, 230–400 mesh). NMR spectra were obtained on a Bruker Avance II 400 at an operating frequency of 400 MHz for ^{1}H, using the solvent peak as internal reference. The solvent is indicated in parenthesis before the chemical shift values (δ relative to TMS). Peak assignments were made by comparison of chemical shifts, peak multiplicities and J values. UV-vis absorption spectra were obtained using a Shimadzu UV/2501PC spectrophotometer. Fluorescence spectra were collected using a FluoroMax-4 spectrofluorometer. The relative fluorescence quantum yields were determined using fluorescein in a 0.1M aqueous solution of NaOH (ϕ_F = 0.79) [22]. Mass spectrometry analysis were performed at the C.A.C.T.I. – Unidad de Espectrometria de Masas of the University of Vigo, Spain.

4.3. General procedure for the synthesis of cyanoacetic arylbithiophene derivatives **2a-d** through Knoevenagel condensation

One drop of piperidine was added to a solution of the appropriate aldehydes **1a-d** (2.5 mmol) and 2-cyanoacetic acid (3 mmol) in acetonitrile. The mixture was refluxed for 2–3 h then cooled down to 0 °C. The precipitate was filtered and washed with ethyl ether to give the pure products.

4.3.1. 2-Cyano-3-(5″-phenyl-2′,2″-bithiophen-5′-yl)acetic acid (**2a**)

Yellow solid (81%). Mp. 179–180 °C. IR (nujol) ν 3335 (O-H), 2207 (C≡N), 1658 (C=O) cm^{-1}. λ_{max}(dioxane)/nm 430 ε/dm^3 mol^{-1} cm^{-1} 27,249.^{1}H NMR (C*D*Cl$_3$, 300 MHz) δ 7.34 (m, 1H, 4‴-*H*), 7.42 (m, 2H, 3‴ and 5‴-*H*), 7.47 (d, 1H, J = 3.9 Hz, 4′-*H*), 7.96 (d, 1H, J = 3.9 Hz, 3″-*H*), 7.57 (d, 1H, J = 3.9 Hz, 3′-*H*), 7.69 (m, 3H, 2‴, 6‴ and 4″-*H*), 8.64 (s, 1H, C*H*$_{vinylic}$), 9.00 (s, 1H, COO*H*) ppm. ^{13}C RMN (DMSO-d_6, 75.4 MHz) δ 79.1, 108.8, 119.1, 124.5, 125.2, 126.9, 128.2, 129.3, 132.9, 134.8, 135.8, 136.8, 140.4, 141.3, 143.9, 163.4 ppm. MS (microTOF) m/z (%) = 338 ([M+1]$^+$, 100), 318 (33), 305 (32), 296 (29), 284 (20), 261 (15), 245 (15), 217 (16), 201 (64), 158 (22). HRMS: m/z (microTOF) [M+1]$^+$ found 338.0312; $C_{18}H_{11}NO_2S_2$ requires 338.0304.

4.3.2. 2-Cyano-3-(5″-(4‴-N,N-dimethylaminophenyl)-2′,2″-bithiophen-5′-yl)acetic acid (**2b**)

Red solid (40%). Mp. 219–221 °C. IR (nujol) ν 2199 (C≡N), 1655 (C=O) cm^{-1}. λ_{max}(dioxane)/nm 466 ε/dm^3 mol^{-1} cm^{-1} 21,008.^{1}H NMR (C*D*Cl$_3$, 300 MHz) δ 2.94 (s, 6H, N(C*H*$_3$)$_2$), 6.73 (d, 2H, J = 9.0 Hz, 3‴ and 5‴-*H*), 7.30 (d, 1H, J = 3.9 Hz, 4′-*H*), 7.37 (d, 1H, J = 3.9 Hz, 3″-*H*), 7.40 (d, 1H, J = 3.9 Hz, 3″-*H*), 7.51 (d, 2H, J = 9.0 Hz, 2‴ and 6‴-*H*), 7.64 (d, 1H, J = 3.9 Hz, 4″-*H*), 8.03 (s, 1H, C*H*$_{vinylic}$), 8.90 (s, 1H, COO*H*) ppm. ^{13}C RMN (DMSO-d_6, 75.4 MHz) δ 39.8, 108.8, 112.3, 119.3, 120.7, 122.2, 123.6, 126.3, 126.8, 132.1, 135.1, 136.5, 140.1, 141.7, 145.4, 150.1, 163.2 ppm. MS (microTOF) m/z (%) = 381 ([M+1]$^+$, 100), 359 (10), 312 (4). HRMS: m/z (microTOF) [M+1]$^+$ found 381.0735; $C_{20}H_{16}N_2O_2S_2$ requires 381.0726.

4.3.3. 2-Cyano-3-(5″-(4‴-N,N-ethylaminophenyl)-2′,2″-bithiophen-5′-yl) acetic acid (**2c**)

Red solid (50%). Mp. 171–173 °C. IR (nujol) ν 2201 (C≡N), 1635 (C=O) cm^{-1}. λ_{max}(dioxane)/nm 474 ε/dm^3 mol^{-1} cm^{-1} 20,661.^{1}H NMR (C*D*Cl$_3$, 300 MHz) δ 1,09 (t, 6H, J = 6.9 Hz, N(CH$_2$C*H*$_3$)$_2$), 3.35 (q, 4H, J = 6.9 Hz, N(C*H*$_2$CH$_3$)$_2$), 6.66 (d, 2H, J = 9.0 Hz, 3‴ and 5‴-*H*), 7.26 (d, 1H, J = 3.9 Hz, 4′-*H*), 7.36 (d, 1H, J = 3.9 Hz, 3′-*H*), 7,40 (d, 1H, J = 3.9 Hz, 3″-*H*), 7,46 (d, 2H, J = 9.0 Hz, 2‴ and 6‴-*H*), 7.64 (d, 1H, J = 3.9 Hz, 4″-*H*), 8.03 (s, 1 H, C*H*$_{vinylic}$), 8.90 (s, 1H, COO*H*) ppm. ^{13}C RMN (DMSO-d_6, 75.4 MHz) δ 12.4, 43.7, 108.7, 111.6, 119.3, 119.7, 121.8, 123.5, 126.5, 126.6, 131.8, 135.0, 136.5, 140.2, 141.8, 145.6, 147.4, 163.4 ppm. MS (microTOF) m/z (%) = 409 ([M+1]$^+$, 100), 391 (10), 318 (4). HRMS: m/z (microTOF) [M+1]$^+$ found 409.1055; $C_{22}H_{21}N_2O_2S_2$ requires 409.1039.

4.3.4. 2-Cyano-3-(5″-(4‴-pyrrolidinophenyl)-2′,2″-bithiophen-5′-yl) acetic acid (**2d**)

Red solid (75%). Mp. 214–216 °C. λ_{max}(dioxane)/nm 449 ε/dm^3 mol^{-1} cm^{-1} 22,523.^{1}H NMR (C*D*Cl$_3$, 300 MHz) δ 1.95 (m, 4H, N(CH$_2$C*H*$_3$)$_2$), 3.28 (m, 4H, N(C*H*$_2$CH$_3$)$_2$), 6.57 (d, 2H, J = 8.7 Hz, 3‴ and 5‴-*H*), 7.27 (d, 1H, J = 3.9 Hz, 4′-*H*), 7.36 (d, 1H, J = 4.2 Hz, 3″-*H*), 7.40 (d, 1H, J = 3.9 Hz, 3′-*H*), 7.50 (d, 2H, J = 8.7 Hz, 2‴ and 4‴-*H*), 7.62 (d, 1H, J = 4.2 Hz, 4″-*H*), 8.01 (s, 1 H, C*H*$_{vinylic}$), 8.65 (s, 1H, COO*H*) ppm.

4.4. General procedure for the synthesis of arylbithiophene rhodanine derivatives **3a** and **3c-d** through Knoevenagel condensation

Four drops of piperidine was added to a solution of the appropriate aldehydes **1a** or **1c-d** (2.5 mmol) and rhodanine-3-acetic acid (3 mmol) in ethanol. The mixture was refluxed for 6 h then cooled down to room temperature. The crude product was concentrated and ethyl ether was added to induce precipitation. The precipitate was filtered and washed with ethyl ether to give the pure product.

4.4.1. 2-(5′-((5″-(5‴-Phenyl-2″,2‴-bithiophen-5″-yl)methylene)-4′-oxo-2′-thioxothiazolidin-3′-yl)acetic acid (**3a**)

Orange solid (69%). IR (liquid film): 3360 (O-H), 1581 (C=O), 1275 (C=S) cm^{-1}. λ_{max}(dioxane)/nm 457 ε/dm^3 mol^{-1} cm^{-1} 25,542.^{1}H NMR (DMSO-d_6, 400 MHz) δ 4.52 (s, 2H, C*H*$_2$COOH), 7.33–7.47 (m, 3H, 3‴'-H, 5‴'-H, 4‴-H), 7.57–7.62 (m, 3H, 4″-H, 3‴-H, 4‴-H), 7.71 (d, 2H, J = 8.4 Hz, 2‴'-H, 6‴'-H), 7.76 (d, 1H, J = 4.4 Hz, 3″-H), 8.10 (s, 1H, =C*H*) ppm. MS (ESI) m/z (%) = 443 (30), 379 (53), 271 (100). HRMS: m/z (ESI) [M]$^+$ found 442.9775; $C_{20}H_{13}NO_3S_4$ requires 442.9778.

4.4.2. 2-(5′-(5″-(4‴'-N,N-Diethylaminophenyl)-2″,2‴bithiophen-5″-yl)methylene)-4′-oxo-2′-thioxothiazolidin-3′-yl)acetic acid (**3c**)

Red solid (24%). IR (liquid film): 3363 (O-H), 1585 (C=O), 1279 (C=S) cm^{-1}. λ_{max} (dioxane)/nm 494 ε/M^{-1}cm^{-1} 14,259.^{1}H NMR (DMSO-d_6, 400 MHz) δ 1.13 (m, 6H, N(CH$_2$C*H*$_3$)$_2$), 3.01 (m, 4H, N(C*H*$_2$CH$_3$)$_2$), 4.56 (s, 2H, C*H*$_2$COOH), 6.68 (d, 2H, J = 8.2 Hz, 3‴'-H, 5‴'-H), 7.30 (d, 1H, J = 3.6 Hz, 4‴-H), 7.47-7-53 (m, 4H, 2‴'-H, 6‴'-H, 3‴-H, 3″-H), 7.75 (d, 1H, J = 4.0 Hz, 4″-H), 8.09 (s, 1H, =C*H*) ppm. MS (ESI) m/z (%) = 514 (1), 342 (100), 313 (17). HRMS: m/z (ESI) [M]$^+$ found 514.05078; $C_{24}H_{22}N_2O_3S_4$ requires 514.05133.

4.4.3. 2-(5′-(5″-(4‴'-Pyrrolidinophenyl)-2″,2‴bithiophen-5″-yl) methylene)-4′-oxo-2′-thioxothiazolidin-3′-yl)acetic acid (**3d**)

Black solid (38%). IR (liquid film): 3366 (O-H), 1585 (C=O), 1281 (C=S) cm^{-1}. λ_{max} (dioxane)nm 477 ε/M^{-1}cm^{-1} 10,794.^{1}H NMR (DMSO-d_6, 400 MHz) δ 1.95 (m, 4H, 2 × 3‴''-H, 2 × 4‴''-H), 2.93–2.95 (m, 4H, 2 × 2‴''-H, 2 × 6‴''-H), 4.49 (s, 2H, C*H*$_2$COOH), 6.56 (d, 2H, J = 8.8 Hz, 3‴'-H, 5‴'-H), 7.32 (d, 1H, J = 4.4 Hz, 4‴-H), 7.46–7.53 (m, 3H, 2‴'-H, 6‴'-H, 3‴-H), 7.73 (d, 1H, J = 4.0 Hz, 4″-H), 7.96 (d, 1H, J = 4.4 Hz, 5″-H), 8.07 (s, 1H, =C*H*) ppm. MS (ESI) m/z (%) = 512 (4) 391 (21), 339 (100). HRMS: m/z (ESI) [M]$^+$ found 513.03551; $C_{24}H_{20}N_2O_3S_4$ requires 513.03568.

4.5. Nonlinear optical measurements

Hyper-Rayleigh scattering (HRS) was used to measure the orientationally averaged first hyperpolarizability β of the push-pull chromophores **2a-e** and **3a-d**. The experimental set-up for hyper-Rayleigh scattering measurements is similar to that presented by Clays

and Persoons [18b]. The incident laser beam comes from a Q-switched Nd:YAG laser, operating at a 10 Hz repetition rate with approximately 2 mJ of energy per pulse and a pulse duration (FWHM) close to 12 ns at the fundamental wavelength of 1064 nm. The incident beam is focused into the solution contained in a long cuvette (1 × 5 cm), and its power can be varied using a combination of a half wave plate and Glan polarizer. The hyper-Rayleigh signal is collimated by a high numerical aperture lens, passed through an interference filter with a full width at half maximum transmission of 3.3 nm centered at the second harmonic wavelength (532 nm), and then detected by a photomultiplier (Hamamatsu model H9305-04). The electronic pulses from the photomultiplier were integrated using a Stanford Research Systems gated box-car integrator (model SR250) with a 20 ns gate centered on the temporal position of the incident laser pulse. The hyper-Rayleigh signal was normalized at each pulse using the second harmonic signal from a 1 mm KH_2PO_4 plate to compensate for fluctuations in the temporal profile of the laser pulses due to longitudinal mode beating. 1,4-Dioxane was used as solvent for the compounds, and the β values were calibrated using a solution of *p*-nitroaniline (*p*NA) in 1,4-dioxane (10^{-2} M) as the external reference [23]. The concentrations of the solutions under study were chosen so that the corresponding hyper-Rayleigh signals fall well within the dynamic range of both the photomultiplier and the integrator. All solutions were previously filtered (0.2 μm porosity) to avoid other signals from suspended impurities. Measurements are carried out using two interference filters with different transmission pass bands centered near the second harmonic at 532 nm. The transmission of each filter at the second harmonic wavelength was carefully determined using a crystalline quartz sample: the transmission band for the narrower filter is 1.66 nm (full width at half maximum) with a transmission of 47.6% at the second harmonic; for the wider filter, the transmission band is 3.31 nm, with a transmission of 63.5% at the second harmonic. By comparing the signals obtained by the use of the two filters, the relative contributions of the hyper-Rayleigh and possible fluorescence signals is determined [11b]. Following reference [19b] we have chosen to report our values using the so-called T (Taylor expansion) convention in which the β_{333} of *p*NA in dioxane at 1064 nm is 40×10^{-30} esu. This value includes a correction factor of 1.88 that accounts for the most recent measurement of the CCl_4 hyper-Rayleigh scattering signal which was used as a reference [24]. The standard two-level model that ignores damping was used to estimate the static second-order hyperpolarizability β_0 [20]. Due to the simplicity of the model, these extrapolated values should be treated with some caution.

Acknowledgments

Thanks are due to *Fundação para a Ciência e Tecnologia* (FCT) for a PhD grant to S. S. M. Fernandes (SFRH/BD/87786/2012) and FEDER-COMPETE for financial support through the CQ/UM (Ref. UID/QUI/00686/2013 and UID/QUI/0686/2016). The NMR spectrometer Bruker Avance III 400 is part of the National NMR Network and was purchased within the framework of the National Program for Scientific Re-equipment, contract REDE/1517/RMN/2005 with funds from POCI 2010 (FEDER) and FCT. The pulsed laser system was acquired within the framework of the grant (PTDC/CTM/105597/2008) from the *Fundação para a Ciência e Tecnologia* (FCT) with funding from FEDER-COMPETE. This work was also supported by the Associated Laboratory for Sustainable Chemistry - Clean Processes and Technologies - LAQV which is financed by Portuguese national funds from FCT/MEC (UID/QUI/50006/2013) and co-financed by the ERDF under the PT2020 Partnership Agreement (POCI-01-0145-FEDER–007265).

References

[1] (a) Meier H. Conjugated oligomers with terminal donor-acceptor substitution. Angew Chem Int Ed 2005;44(17):2482–506;
(b) Bureš F. Fundamental aspects of property tuning in push-pull molecules. RSC Adv 2014;4(102):58826–51.
[2] Allard S, Forster M, Souharce B, Thiem H, Scherf U. Organic semiconductors for solution-processable field-effect transistors (OFETs). Angew Chem Int Ed 2008;47(22):4070–98.
[3] Ohmori Y. Development of organic light-emitting diodes for electro-optical integrated devices. Laser Phot Rev 2010;4(2):300–10.
[4] (a) Burland D. Optical nonlinearities in chemistry: introduction. Chem Rev 1994;94(1):1–2;
(b) He GS, Tan L-S, Zheng Q, Prasad PN. Multiphoton absorbing materials: molecular designs, characterizations, and applications. Chem Rev 2008;108(4):1245–330;
(c) Pawlicki M, Collins HA, Denning RG, Anderson HL. Two-photon absorption and the design of two-photon dyes. Angew Chem Int Ed 2009;48(18):3244–66.
[5] Hains AW, Liang Z, Woodhouse MA, Gregg BA. Molecular semiconductors in organic photovoltaic cells. Chem Rev 2010;110(11):6689–735.
[6] (a) Clifford JN, Martinez-Ferrero E, Viterisi A, Palomares E. Sensitizer molecular structure-device efficiency relationship in dye sensitized solar cells. Chem Soc Rev 2011;40(3):1635–46;
(b) Wu Y, Zhu W. Organic sensitizers from D-π-A to D-A-π-A: effect of the internal electron-withdrawing units on molecular absorption, energy levels and photovoltaic performances. Chem Soc Rev 2013;42(5):2039–58.
[7] (a) Walker B, Kim C, Nguyen T-Q. Small molecule solution-processed bulk heterojunction solar cells. Chem Mater 2011;23(3):470–82;
(b) Mishra A, Bäuerle P. Small molecule organic semiconductors on the move: promises for future solar energy technology. Angew Chem Int Ed 2012;51(9):2020–67;
(c) Duan C, Huang F, Cao Y. Recent development of push-pull conjugated polymers for bulk-heterojunction photovoltaics: rational design and fine tailoring of molecular structures. J Mater Chem 2012;22(21):10416–34.
[8] Qian G, Wang ZY. Near-infrared organic compounds and emerging applications. Chem - Asian J 2010;5(5):1006–29.
[9] (a) Klikar M, Solanke P, Tydlitát J, Bureš F. Alphabet-inspired design of (hetero) aromatic push–pull chromophores. Chem Rec 2016;16(4):1886–905;
(b) Choi H, Baik C, Kang SO, Ko J, Kang M-S, Nazeeruddin MK, et al. Highly efficient and thermally stable organic sensitizers for solvent-free dye-sensitized solar cells. Angew Chem Int Ed 2008;47:327–30;
(c) Mishra A, Ma C-Q, Bäuerle P. Functional oligothiophenes: molecular design for multidimensional nanoarchitectures and their applications. Chem Rev 2009;109(3):1141–276;
(d) Cinar ME, Ozturk T. Thienothiophenes, dithienothiophenes, and thienoacenes: syntheses, oligomers, polymers, and properties. Chem Rev 2015;115(9):3036–140.
[10] (a) Raposo MMM, Ferreira AMFP, Belsley M, Moura JCVP. 5'-Alkoxy-2,2'-bithiophene azo dyes: a novel promising series of NLO-chromophores. Tetrahedron 2008;64(25):5878–84;
(b) Batista RMF, Costa SPG, Belsley M, Lodeiro C, Raposo MMM. Synthesis and characterization of novel (oligo)thienyl-imidazo-phenanthrolines as versatile π-conjugated systems for several optical applications. Tetrahedron 2008;64(39):9230–8;
(c) Herbivo C, Comel A, Kirsch G, Fonseca AMC, Belsley M, Raposo MMM. Synthesis and characterization of novel, thermally stable 2-aryl-5-dicyanovinylthiophenes and 5-aryl-5'-dicyanovinyl-2,2'-bithiophenes as potentially promising non-linear optical materials. Dyes Pigments 2010;86(3):217–26;
(d) Raposo MMM, Castro MCR, Belsley M, Fonseca AMC. Push–pull bithiophene azo-chromophores bearing thiazole and benzothiazole acceptor moieties: synthesis and evaluation of their redox and nonlinear optical properties. Dyes Pigments 2011;91(3):454–65;
(e) Genin E, Hugues V, Clermont G, Herbivo C, Castro MCR, Comel A, et al. Fluorescence and two-photon absorption of push-pull aryl(bi)thiophenes: structure-property relationships. Photochem Photobiological Sci 2012;11(11):1756–66;
(f) Castro MCR, Schellenberg P, Belsley M, Fonseca AMC, Fernandes SSM, Raposo MMM. Design, synthesis and evaluation of redox, second order nonlinear optical properties and theoretical DFT studies of novel bithiophene azo dyes functionalized with thiadiazole acceptor groups. Dyes Pigments 2012;95(2):392–9;
(g) Wojciechowski A, Raposo MMM, Castro MCR, Kuznik W, Fuks-Janczarek I, Pokladko-Kowar M, et al. Nonlinear optoelectronic materials formed by push–pull (bi)thiophene derivatives functionalized with di(tri)cyanovinyl acceptor groups. J Mater Sci Mater Electron 2014;25(4):1745–50;
(h) Castro MCR, Belsley M, Raposo MMM. Synthesis and characterization of push–pull bithienylpyrrole NLOphores with enhanced hyperpolarizabilities. Dyes Pigments 2016;131:333–9;
(i) Castro MCR, Belsley M, Raposo MMM. Push–pull second harmonic generation chromophores bearing pyrrole and thiazole heterocycles functionalized with several acceptor moieties: syntheses and characterization. Dyes Pigments 2016;128:89–95.
[11] (a) Garnier F, Horowitz G, Peng X, Fichou D. An all-organic "soft" thin film transistor with very high carrier mobility. Adv Mater 1990;2(12):592–4;
(b) Geiger F, Stoldt M, Schweizer H, Bäuerle P, Umbach E. Electroluminescence from oligothiophene-based light-emitting devices. Adv Mater 1993;5(12):922–5;
(c) Noma N, Tsuzuki T, Shirota Y. α-Thiophene octamer as a new class of photoactive material for photoelectrical conversion. Adv Mater 1995;7(7):647–8;
(d) Hajlaoui R, Fichou D, Horowitz G, Nessakh B, Constant M, Garnier F. Organic transistors using α-octithiophene and α, ω-dihexyl-α-octithiophene: influence of oligomer length versus molecular ordering on mobility. Adv Mater 1997;9(7):557–61;
(e) Casado J, Pappenfus TM, Miller LL, Mann KR, Ortí E, Viruela PM, et al. Nitro-functionalized oligothiophenes as a novel type of electroactive molecular material:

spectroscopic, electrochemical, and computational study. J Am Chem Soc 2003;125(9):2524–34;
(f) Waldauf C, Schilinsky P, Perisutti M, Hauch J, Brabec CJ. Solution-processed organic n-type thin-film transistors. Adv Mater 2003;15(24):2084–8;
(g) Ong BS, Wu Y, Liu P, Gardner S. High-performance semiconducting polythiophenes for organic thin-film transistors. J Am Chem Soc 2004;126(11):3378–9;
(h) Perepichka IF, Perepichka DF, Meng H, Wudl F. Light-emitting polythiophenes. Adv Mater 2005;17(19):2281–305;
(i) Schulze K, Uhrich C, Schüppel R, Leo K, Pfeiffer M, Brier E, et al. Efficient vacuum-deposited organic solar cells based on a new low-bandgap oligothiophene and fullerene C60. Adv Mater 2006;18(21):2872–5;
(j) Facchetti A, Mushrush M, Yoon M-H, Hutchison GR, Ratner MA, Marks TJ. Building blocks for n-type molecular and polymeric electronics. Perfluoroalkyl- versus alkyl-functionalized oligothiophenes (nT; n = 2 − 6). Systematics of thin film microstructure, semiconductor performance, and modeling of majority charge injection in field-effect transistors. J Am Chem Soc 2004;126(42):13859–74.

[12] (a) Fernandes SSM, Castro MCR, Mesquita I, Andrade L, Mendes A, Raposo MMM. Synthesis and characterization of novel thieno[3,2-*b*]thiophene based metal-free organic dyes with different heteroaromatic donor moieties as sensitizers for dye-sensitized solar cells. Dyes Pigments 2017;136:46–53;
(b) Fernandes SSM, Mesquita I, Andrade L, Mendes A, Justino LLG, Burrows HD, et al. Synthesis and characterization of push-pull bithiophene and thieno[3,2-*b*] thiophene derivatives bearing an ethyne linker as sensitizers for dye-sensitized solar cells. Org Electron 2017;49:194–205;
(c) Fernandes SSM, Pereira A, Ivanou D, Mendes A, Raposo MMM. Benzothiadiazole derivatives functionalized with two different (hetero)aromatic donor groups: synthesis and evaluation as TiO_2 sensitizers for DSSCs. Dyes Pigments 2017. in press;
(d) Fernandes SSM, Castro MCR, Pereira A, Ivanou D, Mendes A, Serpa C, et al. Optical and photovoltaic properties of thieno[3,2-*b*]thiophene based push-pull organic dyes with different anchoring groups for dye-sensitized solar cells. ACS Omega 2017. in press.

[13] (a) Castro MCR, Belsley M, Fonseca AMC, Raposo MMM. Synthesis and characterization of novel second-order NLO-chromophores bearing pyrrole as an electron donor group. Tetrahedron 2012;68(39):8147–55;
(b) Garcia-Amorós J, Reig M, Castro MCR, Cuadrado A, Raposo MMM, Velasco D. Molecular photo-oscillators based on highly accelerated heterocyclic azo dyes in nematic liquid crystals. Chem Commun 2014;50(51):6704–6.

[14] (a) Zhang L, Cole JM. Anchoring groups for dye-sensitized solar cells. ACS Appl Mater. Interfaces 2015;7:3427–55;
(b) Wan Z, Jia C, Duan Y, Zhang J, Lin Y, Shi Y. Effects of different acceptors in phenothiazine-triphenylamine dyes on the optical, electrochemical, and photovoltaic properties. Dyes Pigments 2012;94:150–5;
(c) Ramkumar S, Manoharan S, Anandan S. Synthesis of D-$(\pi$-A$)_2$ organic chromophores for dye-sensitized solar cells. Dyes Pigments 2012;94:503–11;
(d) Song J-L, Amaladass P, Wen S-H, Pasunooti KK, Li A, Yu YL, et al. Aryl/heteroarylethyne bridged dyes: the effect of planar π-bridge on the performance of dye-sensitized solar cells. New J Chem 2011;35:127–36;
(e) Ma XM, Wu WJ, Zhang Q, Guo FL, Meng FS. Novel fluoranthene dyes for efficient dye-sensitized solar cells. Dyes Pigmemts 2009;82:353–9;
(f) Marinado T, Hagberg DP, Hedlund M, Edvinsson T, Johansson EMJ, Boschloo G. Rhodanine dyes for dye-sensitized solar cells: spectroscopy, energy levels and photovoltaic performance. Phys Chem Chem Phys 2009;11:133–41.

[15] Herbivo C, Comel A, Kirsch G, Raposo MMM. Synthesis of 5-aryl-5'-formyl-2,2'-bithiophenes as new precursors for nonlinear optical (NLO) materials. Tetrahedron 2009;65(10):2079–86.

[16] Al-Eid M, Lim S, Park K-W, Fitzpatrick B, Han C-H, Kwak K, et al. Facile synthesis of metal-free organic dyes featuring a thienylethynyl spacer for dye sensitized solar cells. Dyes Pigments 2014;104:197–203.

[17] Valeur B, Berberan-Santos MN. Molecular fluorescence: principles and applications. second ed. Weinheim, Germany: Wiley-VCH; 2012.

[18] (a) Clays K, Persoons A. Hyper-Rayleigh scattering in solution. Phys Rev Lett 1991;66(23):2980–3;
(b) Clays K, Persoons A. Hyper-Rayleigh scattering in solution. Rev Sci Instrum 1992;63(6):3285–9.

[19] (a) Kaatz P, Shelton DP. Polarized hyper-Rayleigh light scattering measurements of nonlinear optical chromophores. J Chem Phys 1996;105(10):3918–29;
(b) Reis H. Problems in the comparison of theoretical and experimental hyperpolarizabilities revisited. J Chem Phys 2006;125(1):014506.

[20] (a) Oudar JL. Optical nonlinearities of conjugated molecules: stilbene derivatives and highly polar aromatic compounds. J Chem Phys 1977;67(2):446–57;
(b) Oudar JL, Chemla DS. Hyperpolarizabilities of the nitroanilines and their relations to the excited state dipole moment. J Chem Phys 1977;66(6):2664–8;
(c) Oudar JL, Zyss J. Structural dependence of nonlinear-optical properties of methyl-(2,4-dinitrophenyl)-aminopropanoate crystals. Phys Rev A 1982;26(4):2016–27.

[21] Frisch MJ, Trucks GW, Schlegel HB, Scuseria GE, Robb MA, Cheeseman JR, et al. Gaussian 09, revision B.01. Wallingford CT: Gaussian, Inc.; 2010.

[22] Umberger JQ, LaMer VK. The kinetics of diffusion controlled molecular and ionic reactions in solution as determined by measurements of the quenching of fluorescence. J Am Chem Soc 1945;67:1099–109.

[23] (a) Teng CC, Garito AF. Dispersion of the nonlinear second-order optical susceptibility of organic systems. Phys Rev B 1983;28(12):6766–73;
(b) Stähelin M, Burland DM, Rice JE. Solvent dependence of the second order hyperpolarizability in p-nitroaniline. Chem Phys Lett 1992;191(3):245–50.

[24] Pyatt RD, Shelton DP. Hyper-Rayleigh scattering from CH_4, CD_4, CF_4, and CCl_4. J Chem Phys 2001;114(22):9938–46.